Aquaculture and Fisheries 2 (2017) 34–38

Contents lists available at ScienceDirect

Aquaculture and Fisheries

journal homepage: www.keaipublishing.com/en/journals/aquaculture-and-fisheries/

Original research article

The structure and mechanical property of silane-grafted-polyethylene/SiO_2 nanocomposite fiber rope

Wenwen Yu, Jiangao Shi*, Lumin Wang, Xiaoxue Chen, Minghua Min, Lei Wang, Yongli Liu

East China Sea Fisheries Research Institute, Chinese Academy Fishery Sciences, Shanghai 200090, China

ARTICLE INFO

Article history:
Received 10 May 2016
Received in revised form
1 December 2016
Accepted 30 December 2016
Available online 22 January 2017

Keywords:
Nanocomposite fiber rope
Polyethylene
SiO_2
Mechanical property

ABSTRACT

The effect of vinyltrimethoxysilane (VTMS) graft and SiO_2 on the structure and mechanical properties of silane-grafted-polyethylene/SiO_2 (VTMS-g-PE/SiO_2) nanocomposite fibers and ropes was studied. Scanning electron microscopy (SEM), Fourier transfer infrared (FT-IR), differential scanning calorimetry analysis (DSC) and tensile mechanical tests were performed to characterize the morphology, thermal and mechanical properties of nanocomposite fibers and ropes. The results revealed that the SiO_2 nanoparticles were well dispersed throughout the polymeric matrix. With increasing SiO_2 content, T_m, the melt peak width and X_c, degree of crystallinity, of VTMS-g-PE/SiO_2 nanocomposite fibers increased. The breaking load and breaking strength of the nanocomposite fiber ropes were remarkably improved compared to pure PE fiber ropes and elongation at break was also decreased.
© 2017 Shanghai Ocean University. Published by Elsevier B.V. This is an open access article under the CC BY license (http://creativecommons.org/licenses/by/4.0/).

1. Introduction

Ropes, widely used in modern fishery, are most commonly made of synthesized fibers such as polyethylene (PE) fiber, polypropylene (PP) fiber, polyamide (PA) fiber and polyester (PET) fiber (McKenna, Hearle, & O'Hear, 2004; McKenna, 1983, 2006). Among such materials, PE fiber ropes are the most used thermoplastic commodity for fisheries, due to their good mechanical properties, chemical resistance, low density, processability and low cost (Marissen, 2011). Such ropes are wildly used in lifting and mooring applications in oceanographic research, offshore oil and gas explorations and commercial fishing (Banfield & Casey, 1998; Da Costa Mattos & Chimisso, 2011). PE fiber ropes in particular, are widely used in industrial applications because of the considerable increase in mechanical performance achieved when appropriate mechanical stretching occurs during manufacturing. The tensile mechanical properties of fishing rope have an effect on the expansion, special offshore work and safety against sea wind (McKenna & Wong, 1979; Vlasblom, Boesten, Leite, & Davies, 2012; Wang, Shi, Chen, & Shi, 2009). With the development of modern fisheries, higher performance of synthetic fiber ropes is needed. The mechanical property of general synthetic fiber ropes can't meet the large scale, modernization and special offshore operation requirements of modern fishing and aquaculture operations. Hence, PE fishing ropes with high strength are technologically important and have attracted great interest. High molecular weight polyethylene (UHMWPE) rope has been used successfully in fisheries because of its outstanding comprehensive properties (Ma, Guo, & Mao, 2005; Sheng, Jie, Yang, & Cuo, 2003). At present, it has been applied in marine fishing and large aquatic farm fences. UHMWPE fiber mesh has played an important role in improving the resilience of netting against the effects of ocean waves. However, the large-scale application of UHMWPE fiber in the area of fisheries has been limited by its high costs and complicated gel-spinning technique. Therefore, modified PE fiber ropes with reduced production costs and simplified methods of production are critical for the development of fishing ropes.

The properties of ropes are determined by the properties of their fibers and knitting structure. Modified PE fibers have been extensively studied (Fambri, Dabrowska, Ferrara, & Pegoretti, 2016; Kageyama, Tamazawa, & Aida, 1999; Sulong, Park, Azhari, & Jusoff, 2011; Zhao et al., 2015). Pure PE properties can also be improved through the formulation of nanocomposites taking advantage of the synergistic combination of polymer and nanofiller properties (Alonso et al., 2015; Kutlu et al., 2014; La Mantia, Dintcheva, Scaffaro, & Marino, 2008; Rattanawijan & Amornsakchai, 2012). Alonso et al. (2015) studied the influence of sepiolite content (1, 2, and 3 wt%) and successive drawing steps on the final properties of polyethylene/sepiolite nanocomposite fibers.

* Corresponding author. 300 Jungong Road, Yangpu District, Shanghai 200090, China.
E-mail address: jiangaoshi666@163.com (J. Shi).

http://dx.doi.org/10.1016/j.aaf.2017.01.003
2468-550X/© 2017 Shanghai Ocean University. Published by Elsevier B.V. This is an open access article under the CC BY license (http://creativecommons.org/licenses/by/4.0/).

They found that the Young Modulus increased 17 times with drawing in pure PE fibers and was further enhanced 1.5 times when sepiolite was present and a similar effect on strength was also found. Most published studies have reported that rigid fillers in composite systems, including filled polyethylene, improve the mechanical properties of PE fibers (Fouad, Mourad, & Barton, 2005; Tanaka, 2001). The improvement in the mechanical properties of reinforced materials depends on the dispersed states of the nano-fillers and the interactions between polymer and nano-fillers. To facilitate interactions between polymer and nano-fillers, a polymer functionalized with polar groups, such as maleic anhydride or hydroxyl groups has often been employed. Silanes used in the manufacture of crosslinkable polyolefins are mainly vinyl-alkoxysilane and contain two functional groups in their chemical structures, a C=C group that can be grafted onto polymer and a Si≡OR (R: CH_3 or CH_2CH_3) that can be coupled with nano-fillers (Azizi, Morshedian, & Barikani, 2009; Fabris, Cardozo, Mauler, & Nachtigall, 2009; Lu, Hu, Li, Chen, & Fan, 2006; Sirisinha, Boonkongkaew, & Kositchaiyong, 2010).

In the present study, the morphology, thermal and mechanical properties of a silane-grafted-polyethylene/SiO_2 (VTMS-g-PE/SiO_2) hybrid nanocomposite fiber prepared by reactive extrusion in a twin-screw extruder coupled with melt spinning were investigated. The VTMS-g-PE/SiO_2 nanocomposite fiber rope had a diameter of 10 mm and was made via ring twist and strand combine. The morphology and thermal properties of the nanocomposite fiber rope were characterized by scanning electron microscopy (SEM), Fourier transfer infrared (FTIR) and differential scanning calorimetry analysis (DSC).

2. Materials and methods

2.1. Materials

High density polyethylene (HDPE 5000S) with an MFI 0.9 g per 10 min and density 950 kg/m^3 was supplied by Sinopec Yangzi Petrochemical Company, China. The initiator dicumyl peroxide (DCP), styrene, and vinyltrimethoxysilane (VTMS) were supplied by Sinopharm Chemical Reagent Company, China. The organically modified SiO_2 was provided from Hangzhou Wanjing New Material Company, China.

2.2. Preparation of VTMS-g-PE/SiO_2 nanocomposite fibers

VTMS-g-PE/SiO_2 hybrid was prepared by reactive extrusion in a twin-screw extruder (Jiangsu, China) at 160–220 °C from HDPE (dried at 80 °C for 12 h) with 0.1 phr (part of reagent per hundred parts of HDPE) DCP, 2.0 phr VTMS, 0.1 phr styrene and a pre-determined amount of organically modified SiO_2 (dried at 80 °C for 12 h). The mixing speed was 60 rpm. The extruded strands were pelletized and dried at 80 °C for 24 h to prepare the VTMS-g-PE/SiO_2 hybrid.

The VTMS-g-PE/SiO_2 hybrid was then melt-spun through a 0.5 mm diameter spinneret using a SJ-45C Fiber Spin Line equipped with two drawing roll and a collecting roll. The drawn ratio was 8.0, and the diameter of VTMS-g-PE/SiO_2 nanocomposite fiber was about 0.2 mm. Crosslinking of the grafted samples was performed by immersing the moulded samples in hot water at 90 °C for 48 h under tension. In the present study, several weight ratios of SiO_2 to VTMS-g-PE/SiO_2 nanocomposite fibers were used, 0.3 wt%, 0.5 wt%, and 1 wt% and named VTMS-g-PE/SiO_2-0.3, VTMS-g-PE/SiO_2-0.5 and VTMS-g-PE/SiO_2-1, respectively.

2.3. Preparation of VTMS-g-PE/SiO_2 nanocomposite fiber ropes

A VTMS-g-PE/SiO_2 nanocomposite fiber rope with 3-strand was prepared using a rope twisting machine. The VTMS-g-PE/SiO_2 nanocomposite fiber was first divided and then made into strands. The strands were twisted with VTMS-g-PE/SiO_2 nanocomposite fiber strings and then a number of strands turned around the core to form a twisted rope. The twist was 20 T/m. For comparison purposes, normal 3-strand PE rope and 4-strand twisted PE rope were made as per usual using pure PE fibers.

2.4. Characterization

The microstructures of the fibers were examined using a JEOL 6360LA scanning electron microscope (SEM) (JEOL Ltd., Japan) operated at an acceleration voltage of 15 kV.

FT-IR spectra were measured using a Nicolet spectrometer model 560 (Nicolet Instruments, USA). The samples were scanned 32 times at a resolution of 4 cm^{-1}.

Differential scanning calorimetry (DSC) was applied to investigate the melting and crystallisation behaviour of the fibers using a DSC thermal analyser (204F1, Netzsch Instruments, Germany). The samples were scanned at a heating and cooling rate of 10 °C/min in a nitrogen atmosphere. The degree of crystallinity (X_c) was calculated via the total enthalpy method, using the following equation:

$$X_c = \left(\frac{\Delta H_f^{obs}}{\Delta H_f^0}\right) \times 100 \quad (1)$$

where ΔH_f^{obs} is the observed heat of fusion values; ΔH_f^0 is the specific enthalpy of melting for 100% crystalline polymer and ΔH_f^0 was defined as HDPE 288 J/g.

The tensile properties of VTMS-g-PE/SiO_2 nanocomposite fiber were studied on an Electron Omnipotence Experiment Machine INSTRON-4466 (Instron Instruments, USA) under ambient conditions. The cross-head speed of fibers was 300 mm/min according to SC/T 5005-2014. The cross-head speed of ropes was 100 mm/min according to GB/T 8834-2006. At least five specimens were measured for each of the VTMS-g-PE/SiO_2 (0.3 wt%, 0.5 wt%, and 1 wt%) nanocomposite fiber samples fabricated.

3. Results

3.1. Grafting analysis from FT-IR and morphology of VTMS-g-PE/SiO_2 nanocomposite fibers

Fig. 1 shows the FTIR spectra of HDPE and VTMS-g-PE. All samples displayed characteristic IR peaks at 720 and 1458 cm^{-1} which were assigned to the CH_2 rocking and CH bending vibrations of methyl and methylene groups, respectively. Three additional peaks of methoxysilane (Si–OCH_3) groups were evident at 802, 1092 and 1192 cm^{-1} in the silane-grafted VTMS-g-PE samples (Ahmed, Gilbert, Mainprize, & Rogerson, 2013; Kuan, Kuan, Ma, & Huang, 2005; Lu et al., 2006). The identification of characteristic methoxysilane spectra in all grafted samples confirmed the success of the silane grafting reaction.

Fig. 2 presents the SEM micrographs of VTMS-g-PE/SiO_2-0.5 nanocomposite fibers (Fig. 2a) and their fracture surface (Fig. 2b). The nanocomposite fiber had a smooth surface and the SEM images of the fracture surface indicated that the SiO_2 nanoparticles were well dispersed throughout the polymeric matrix (Fig. 2b).

Fig. 3 shows the DSC heating and cooling thermograms of various VTMS-g-PE/SiO_2 nanocomposite fibers. The DSC data are summarized in Table 1 and includes the melting temperature (T_m),

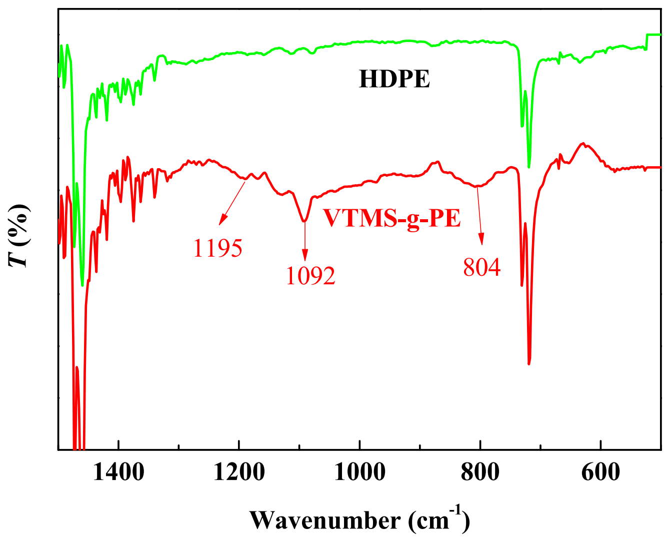

Fig. 1. FTIR spectra of HDPE and VTMS-g-PE.

(ktex) than pure PE fiber ropes. The breaking load of the VTMS-g-PE/SiO_2 nanocomposite fiber rope was improved by 21.2% relative to the 3-strand PE fiber rope and its linear density and the raw material consumption was also 2.7% lower. Comparison of the VTMS-g-PE/SiO_2 nanocomposite fiber rope with 4-strand PE fiber rope, revealed the breaking load was improved by 8.4%, and the linear density and the raw material consumption was reduced by 5.0%.

As shown in Table 2, the VTMS-g-PE/SiO_2 nanocomposite fiber rope had higher breaking strength and lower elongation than pure PE fiber ropes. The breaking strength of VTMS-g-PE/SiO_2 nanocomposite fiber rope of the same diameter as 3-strand PE fiber rope was 34.5% higher.

4. Discussion

VTMS-g-PE/SiO_2 nanocomposite fibers were prepared by reactive extrusion in a twin-screw extruder and melt spinning. FT-IR and SEM results suggests that strong interactions occurred between PE molecular chain and nano-fillers. The reduction in T_m, ΔH_f^{obs} and degree of crystallinity with the introduction of VTMS could be due to some difficulty in chain crystallisation brought about by the presence of the silane crosslink network in the nanocomposite fibers systems. With increasing SiO_2 content, T_m, the melt peak width and X_c of VTMS-g-PE/SiO_2 nanocomposite fibers increased. This means that the nucleating effect of SiO_2 increased the nucleating and crystallizing rate and this resulted in an improvement of T_m and the degree of crystallinity. Increasing SiO_2 content in VTMS-g-PE/SiO_2 nanocomposite fibers caused smaller and more heterogeneous spherulites of PE, which resulted in an increased melt peak width of nanocomposite fibers.

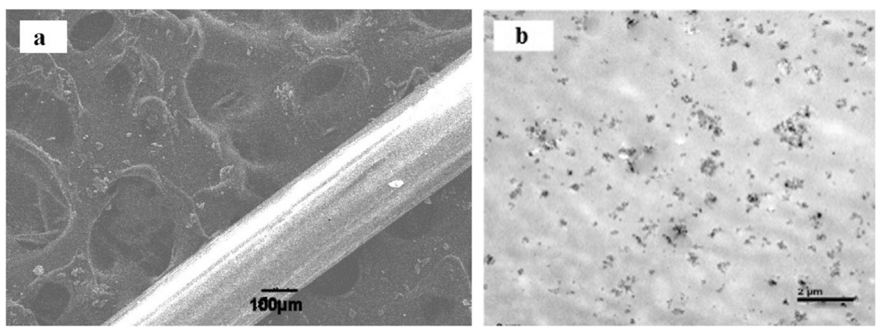

Fig. 2. The surface (a) and cross-session (b) SEM micrographs of VTMS-g-PE/SiO_2-0.5 nanocomposite fiber. Thermal analysis of VTMS-g-PE/SiO_2 nanocomposite fibers.

enthalpy of fusion (ΔH_f^{obs}), X_c and crystallisation temperature (T_c). All VTMS-g-PE/SiO_2 nanocomposite fibers exhibited a melting peak of the HDPE component around 130 °C (Fig. 3a) and the incorporation of VTMS caused a reduction in T_m, ΔH_f^{obs} and degree of crystallinity of HDPE. With increasing SiO_2 content, T_m, the melt peak width and X_c of VTMS-g-PE/SiO_2 nanocomposite fibers increased.

The tensile mechanical properties of VTMS-g-PE/SiO_2 nanocomposite fibers are shown in Fig. 4. The breaking strength of VTMS-g-PE/SiO_2 nanocomposite fibers increased with increasing SiO_2 content and elongation at break decreased monotonically with the addition of nano SiO_2.

VTMS-g-PE/SiO_2 nanocomposite fiber ropes of 10 mm diameter were prepared using VTMS-g-PE/SiO_2-1 nanocomposite fibers as the basal fiber. The tensile mechanical properties of ropes have a direct effect on the security, strength, deformation and service life in modern fishing and aquaculture equipment and engineering (such as trawling fishing gear, deep-water cages and large-scale aquaculture seine, etc.). Breaking load is one of the most important tensile mechanical properties of fishing ropes and it is an important indicator used to assess fishing rope material quality. The comparison of tensile mechanical properties between the VTMS-g-PE/SiO_2 nanocomposite fiber rope and pure PE fiber ropes are shown in Table 2. There was a significant difference in tensile mechanical properties of VTMS-g-PE/SiO_2 nanocomposite fiber ropes and pure PE fiber ropes. The VTMS-g-PE/SiO_2 nanocomposite fiber rope had a greater breaking load and lower linear density

The microstructure transformation of VTMS-g-PE/SiO_2 nanocomposite fibers influenced their mechanical properties and the breaking strength increased with increasing SiO_2 content. This is probably due to the higher degree of crystallinity and the strong interaction between the PE molecular chain and nano SiO_2, which blocked crack propagation and passivated the stretching process. Fabris et al. (2009) also observed increased tensile strength values for silanized-low density polyethylene/glass fiber composites that had increased glass fiber loading. The decrease in elongation at break in the present study indicated that the fiber toughness and cross-linking reaction between nano SiO_2 and grafted VTMS was reduced with increased SiO_2 content.

If the VTMS-g-PE/SiO_2 nanocomposite fiber rope is used to replace currently used 3-strand PE fiber rope or 4-strand PE fiber rope, the breaking load will be improved along with the linear density and raw material consumption can also be reduced. Taken

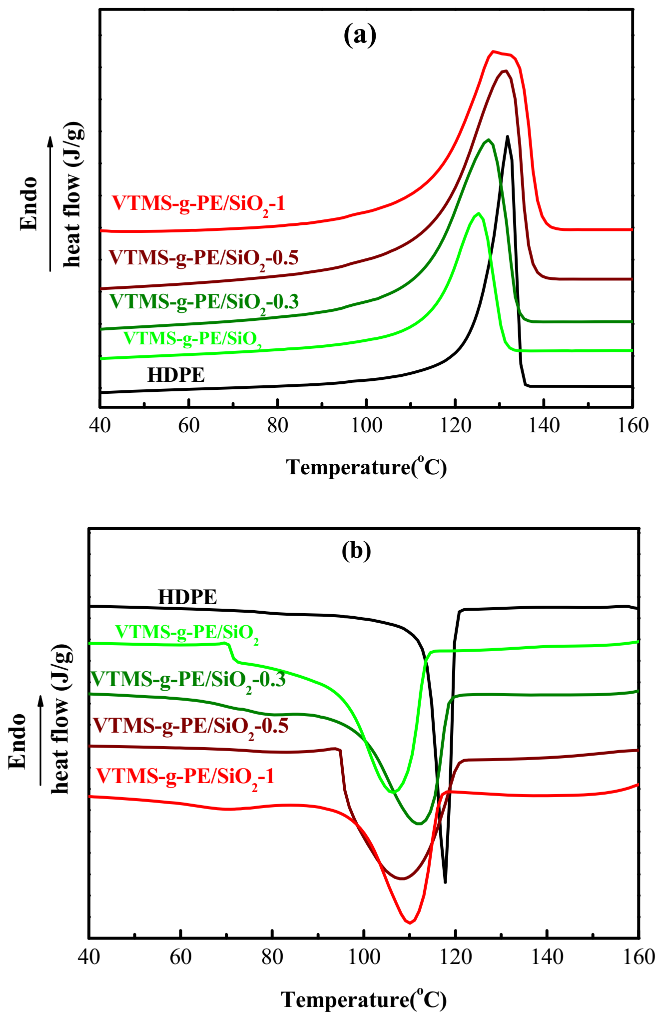

Fig. 3. (a) DSC heating and (b) DSC cooling thermograms of HDPE and VTMS-g-PE/SiO_2 nanocomposite fibers.

Table 1
The DSC data of HDPE and VTMS-g-PE/SiO_2 nanocomposite fibers.

Samples	T_m [°C]	ΔH_f^{obs} [J/g]	X_c [%]	T_c [°C]
HDPE	130.9	197.2	68.5	117.0
VTMS-g-PE	125.3	128.3	44.5	106.3
VTMS-g-PE/SiO_2-0.3	127.5	160.1	55.6	112.0
VTMS-g-PE/SiO_2-0.5	131.1	188.7	65.5	108.4
VTMS-g-PE/SiO_2-1.0	131.2	169.6	58.9	111.4

Tensile mechanical properties of VTMS-g-PE/SiO_2 nanocomposite fibers.

together, these results indicate that VTMS-g-PE/SiO_2 nanocomposite fiber ropes could be used to improve the safety of netting, resulting in greater resilience in aquaculture applications, as well as reduced hydrodynamic drag which can reduce the energy consumption of mobile fishing vessels.

5. Conclusions

In this work, the influence of VTMS graft and SiO_2 on the structure and mechanical properties of VTMS-g-PE/SiO_2 nanocomposite fiber and ropes was determined. SEM images revealed that nano SiO_2 particles were well dispersed throughout the PE matrix. DSC tests revealed a reduction of melting temperature, heat of fusion, and the degree of crystallinity by the grafted VTMS introduction. The T_m, the melt peak width and X_c of nanocomposite fibers increased with increasing SiO_2 content. The tensile mechanical test showed that the breaking strength of the nanocomposite fiber ropes was remarkably improved upon nanofiller addition, with a decrease in the elongation at break. Hence, VTMS-g-PE/SiO_2 nanocomposite fiber rope can take the place of pure PE fiber ropes, and will reduce rope linear density, elongation at break and raw material consumption, while increasing net resistance and security. The study provides a reference for production and processing of ropes, and structure optimization and contributes to the design of modern fisheries equipment and engineering.

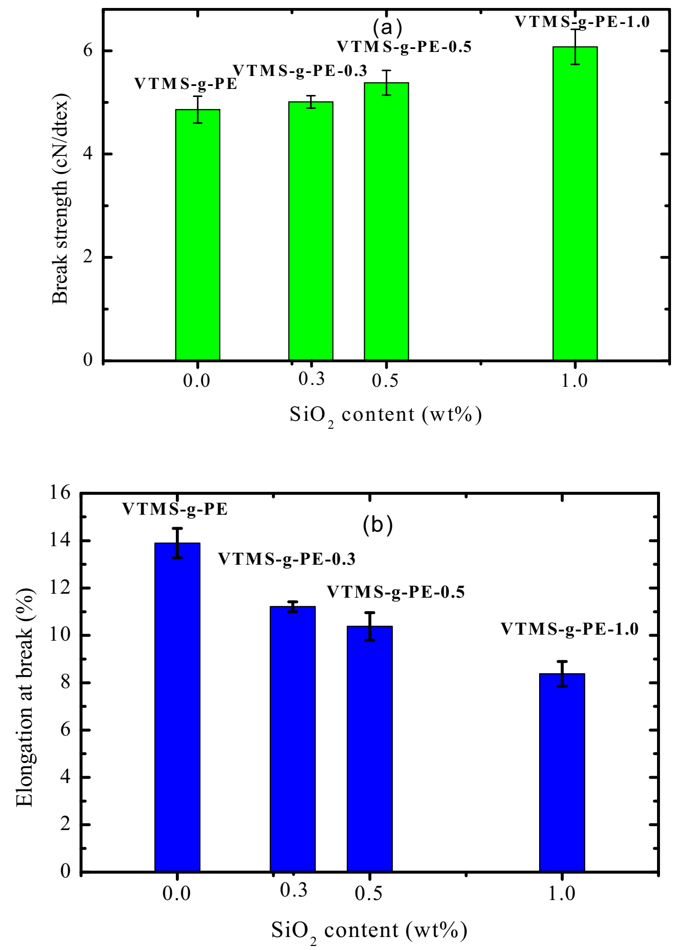

Fig. 4. The tensile mechanical properties of VTMS-g-PE/SiO_2 nanocomposite fibers. Tensile mechanical properties of VTMS-g-PE/SiO_2 nanocomposite fiber rope.

Table 2
Tensile mechanical properties of VTMS-g-PE/SiO_2 nanocomposite fiber rope and pure PE fiber ropes.

Rope types	Diameter (mm)	Linear density (ktex)	Breaking load (kN)	Breaking strength (cN/dtex)	Elongation (%)
VTMS-g-PE/SiO_2 nanocomposite fiber rope	10	47.5	10.3	2.9	35
3-strand PE fiber rope	10	48.8	8.5	1.8	46
4-strand PE fiber rope	10	50.0	9.5	1.9	49

Acknowledgements

This work was supported by the National Natural Science Foundation of China (Grant No. 31502213), Special Scientific Research Funds for Central Non-profit Institutes (East China Sea Fisheries Research Institute) (Grant No. 2015T01) and the National Key Technology R&D Program (Grant No. 2013BAD13B02).

References

Ahmed, G. S., Gilbert, M., Mainprize, S., & Rogerson, M. (2013). FTIR analysis of silane grafted high density polyethylene. *Plastics Rubber and Composites, 38*, 13–20.

Alonso, Y., Martini, R. E., Iannoni, A., Terenzi, A., Kenny, J. M., & Barbosa, S. E. (2015). Polyethylene/sepiolite fibers. Influence of drawing and nanofiller content on the crystal morphology and mechanical properties. *Polymer Engineering & Science, 55*(5), 1096–1103.

Azizi, H., Morshedian, J., & Barikani, M. (2009). Silane grafting and moisture crosslinking of polyethylene: The effect of molecular structure. *Journal of Vinyl and Additive Technology, 15*(3), 184–190.

Banfield, S., & Casey, N. (1998). Evaluation of fibre rope properties for offshore mooring. *Ocean Engineering, 25*(10), 861–879.

Da Costa Mattos, H. S., & Chimisso, F. E. G. (2011). Modelling creep tests in HMPE fibres used in ultra-deep-sea mooring ropes. *International Journal of Solids and Structures, 48*(1), 144–152.

Fabris, F. W., Cardozo, N. S., Mauler, R. S., & Nachtigall, S. (2009). Improving the properties of LDPE/glass fiber composites with silanized-LDPE. *Polymer Composites, 30*(7), 872–879.

Fambri, L., Dabrowska, I., Ferrara, G., & Pegoretti, A. (2016). Morphology and viscoelastic properties of melt-spun HDPE/hydrotalcite nanocomposite fibers. *Polymer Composites, 37*(1), 288–298.

Fouad, H., Mourad, A. H., & Barton, D. C. (2005). Effect of pre-heat treatment on the static and dynamic thermo-mechanical properties of ultra-high molecular weight polyethylene. *Polymer Testing, 24*(5), 549–556.

Kageyama, K., Tamazawa, J. I., & Aida, T. (1999). Extrusion polymerization: Catalyzed synthesis of crystalline linear polyethylene nanofibers within a mesoporous silica. *Science, 285*(5436), 2113–2115.

Kuan, H. C., Kuan, J. F., Ma, C. C. M., & Huang, J. M. (2005). Thermal and mechanical properties of silane-grafted water crosslinked polyethylene. *Journal of Applied Polymer Science, 96*(6), 2383–2391.

Kutlu, B., Meinl, J., Leuteritz, A., Brünig, H., Wießner, S., & Heinrich, G. (2014). Up-scaling of melt-spun LDH/HDPE nanocomposites. *Macromolecular Materials and Engineering, 299*(7), 825–833.

La Mantia, F. P., Dintcheva, N. T., Scaffaro, R., & Marino, R. (2008). Morphology and properties of polyethylene/clay nanocomposite drawn fibers. *Macromolecular Materials and Engineering, 293*(1), 83–91.

Lu, H., Hu, Y., Li, M., Chen, Z., & Fan, W. (2006). Structure characteristics and thermal properties of silane-grafted-polyethylene/clay nanocomposite prepared by reactive extrusion. *Composites Science and Technology, 66*(15), 3035–3039.

Ma, H. Y., Guo, Y. P., & Mao, L. S. (2005). Composite UHMWPE ropes used in the anti-wind-waves cage. *Marine Tieheries, 2*(27), 154–158.

Marissen, R. (2011). Design with ultra strong polyethylene fibers. *Materials Sciences and Applications, 2*(05), 319–330.

McKenna, H. A. (1983). Developments in fiber rope technology. Developments in Fiber Rope Technology. In *Proceedings of the OCEANS'83* (pp. 527–533). Proceedings.

McKenna, H. A. (2006). Fiber rope and fishing. *Marine Technology Society Journal, 40*(3), 40–43.

McKenna, H. A., Hearle, J. W. S., & O'Hear, N. (2004). *Handbook of fibre rope technology*. BocaRaton: CRC Press.

McKenna, H. A., & Wong, R. (1979). Synthetic fiber rope, properties and calculations relating to mooring systems, OED volume 7: Deepwater mooring and drilling. In *Symposium presented at the ASME winter annual meeting, New York* (pp. 2–7).

Rattanawijan, W., & Amornsakchai, T. (2012). Polyethylene composite fibers. I. Composite fibers of high-density polyethylene. *Journal of Applied Polymer Science, 124*(1), 501–509.

Sheng, H. L., Jie, L. W., Yang, H., & Cuo, Z. L. (2003). Study on high strength rope of uhmwpe fibers. *Engineering Plastics Application, 6*, 33–35.

Sirisinha, K., Boonkongkaew, M., & Kositchaiyong, S. (2010). The effect of silane carriers on silane grafting of high-density polyethylene and properties of crosslinked products. *Polymer Testing, 29*(8), 958–965.

Sulong, A. B., Park, J., Azhari, C. H., & Jusoff, K. (2011). Process optimization of melt spinning and mechanical strength enhancement of functionalized multi-walled carbon nanotubes reinforcing polyethylene fibers. *Composites Part B: Engineering, 42*(1), 11–17.

Tanaka, A. (2001). Dynamic mechanical properties of metallocene catalyzed linear polyethylenes. *Polymer, 42*(3), 1219–1226.

Vlasblom, M. P., Boesten, J., Leite, S., & Davies, P. (2012). *New polyethylene fiber suitable for deepwater mooring ropes, 72(8)*. Tulsa: Offshore.

Wang, L. M., Shi, J. G., Chen, X. L., & Shi, H. (2009). Comparative test on the tensile mechanical properties of high-strength polyethylene and common polyethylene braided netting twine for fishing. *Progress in Fishery Sciences, 3*(30), 125–130.

Zhao, Y., Wang, L., Yu, H., Li, C., Jing, G., Tong, R., et al. (2015). Study on the preparation of hyperbranched polyethylene fibers and hyperbranched polyethylene composite fibers via electrospinning. *Journal of Applied Polymer Science, 132*(37), 42517–42528.